Carbon coating may expedite the fracture of carbon-coated silicon core-shell nanoparticles during lithiation†

Weiqun Li,[a] Ke Cao,[b] Hongtao Wang,[c] Jiabin Liu,[b] Limin Zhou,[a] Haimin Yao*,[a]

Previous studies on silicon (Si) indicate the lithiation-induced fracture of crystalline Si nanoparticles can be greatly inhibited if their diameter is reduced to below a critical length scale around 150 nm. In this paper, *in situ* lithiation of individual carbon-coated Si nanoparticles (Si@C NPs) is conducted and shows that Si@C NPs will fracture during lithiation even though the diameter is much smaller than 150 nm, implying a deleterious effect of the carbon coating on the integrity of the Si@C NPs during lithiation. To shed light on this effect, finite element analysis is carried out and reveals that the carbon coating, if fractured during lithiation, will induce cracks terminating at the C/Si interface. Such cracks, upon further lithiation, can immediately propagate into the Si core due to the elevated driving force caused by material inhomogeneity between the coating and core. To prevent the fracture of the carbon coating so as to protect the Si core, a design guideline is proposed by controlling the ratio between the diameter of Si core and the thickness of carbon coating. The results in this paper should be of practical value to the

[a] *Department of Mechanical Engineering, The Hong Kong Polytechnic University, Hung Hom, Kowloon, Hong Kong SAR, P.R. China. E-mail: mmhyao@polyu.edu.hk; Fax: +852-2365 4703; Tel: +852-2766 7817*

[b] *School of Materials Science and Engineering, Zhejiang University, Hangzhou 310027, P.R. China*

[c] *Institute of Applied Mechanics, Zhejiang University, Hangzhou 310027, P.R. China*

† Electronic Supplementary Information (ESI) available: details of finite element simulations including analogous treatment of lithiation-induced expansion, calculation of energy release rate and effect of material's inhomogeneity on it.

design and application of Si-based core-shell structured anode materials for lithium ion batteries.

1. Introduction

Recently, techniques for storage of electrical energy have been developing rapidly, leading to a wide application in many fields such as portable electronic devices, electric vehicles and so on. Lithium ion battery (LIB), due to its high energy density, is recognized as the one of the most promising devices for electrical energy storage.[1] Among diverse electrode materials for LIB, silicon (Si) stands out for its high capacity (~ 4200 mAh g^{-1}), abundant reserves (~28% of the total mass of the earth's crust) and low cost.[2] However, the wide application of Si as the electrode material of LIB is still impeded by its Achilles' heel: the large volume expansion (~400%) during lithiation and delithiation which will cause the fracture and pulverization of the electrode materials and delamination of the interface between the electrode material and periphery structures such as current collector, resulting in poor conductivity and rate capability, short cycle life and even overall failure of the battery.[3,4] Although nanoscale Si particles have been shown to have the capability to resist fracture during lithiation,[5,6] the large volume change of Si electrode would cause repeated fracture and formation of the solid-electrolyte interphase (SEI) layer on the Si electrode surface during lithiation and delithiation. This process not only leads to the thickening of the SEI layer therefore lowers the electronic and ionic conductivity and coulombic efficiency, but also consumes the Si and electrolyte and finally results in the dry-out of the cell.[7] To solve these problems, coating such as carbon has been imposed on the Si to constrain its volume expansion and also prevent the direct contact between the Si and the electrolyte.[8-14] As a

consequence, the electronic and ionic conductivity is improved and a much more stable SEI film forms on the carbon coating surface as long as the structural integrity of coating is maintained. Otherwise, if the carbon coating is cracked during electrochemical cycling, the coating will lose its efficacy as new SEI layer will form and thicken on the electrode surfaces. Therefore, maintaining the structural integrity of carbon coating on the Si electrode materials is significantly important for the application of the carbon-coated Si nanoparticles (Si@C NPs) as the electrode materials for LIB.

In this paper, Si@C NPs were synthesized, on which *in situ* lithiation tests were conducted using transmission electron microscopy (TEM).[15,16] The Si@C NPs were found to fracture even though the diameter of the crystalline Si core is much lower than 150 nm, which has been deemed as the maximum size of bare crystalline Si NPs capable of maintaining integrity during lithiation.[5] Finite element simulation[17-19] was used to account for such deleterious effect of carbon coating on the structural integrity of Si@C NPs, giving rise to a guideline for designing Si@C NPs with high persistence to structural integrity during lithiation.

2. Experimental

2.1. Synthesis of carbon-coated silicon nanoparticles

Si@C NPs were synthesized by using sucrose as the carbon source.[20] 100 mg Si NPs and 600 mg sucrose were firstly dissolved in a solution made of 0.6 mL hydrochloric acid (37 wt%), 6 mL deionized water and 8 mL absolute ethanol (99.9 wt%) under stirring and then ultrasonicated for 120 mins. Subsequently, the solution was stirred at 70 °C for 3 hours and then dried in vacuum oven at 120 °C for 8 hours. The as-prepared Si-sucrose product was loaded in an alumina crucible after manual grinding. Then, the

crucible was moved into the furnace and heated at 800 °C for 2 hours and cooled down to room temperature under the protection of nitrogen atmosphere.

2.2. In situ TEM observation

The *in situ* lithiation test was conducted on the Si@C NPs in a TEM (JEM-2100, JEOL) equipped with a Nanofactory® STM-TEM holder. Fig. 1a shows the schematic of the nanoscale battery setup of the solid electrochemical cell for lithiation,[4-6] in which the Si@C NPs are attached onto the flat-ended gold rod (~200 μm in diameter) with silver paste. To improve the electronic conductivity, a small amount of carbon nanotubes (CNT) were added into the Si@C NPs. The counter electrode was a piezo-driven tungsten probe covered with Li metals. The surface layer of the Li metal was unavoidably oxidized to Li_2O during the handling in air and the resulting Li_2O layer served as solid electrolyte. The intensity of electron beam was minimized to avoid the decomposition of Li_2O layer, prevent the direct contact between the Li metal and the Si@C NPs and therefore guarantee the electrochemical reaction rather than the chemical reaction between Li and Si@C NPs.[5] With the aid of TEM, a nano contact was made between the Li metal and the Si@C NPs and a larger external bias (–3 V), in comparison with that in the actual LIB, was then applied to initiate the lithiation, leading to the Li^+ transportation through the Li_2O layer, the insertion of Li^+ into the carbon coating and then into the Si core, and the phase transition from Si to lithiated Si.[21] The electrochemical reaction and the diffusion of Li^+ here are similar to those in the actual LIB.[4,6] Therefore, the nano battery can effectively simulate the real reaction and structural change in the actual LIB.

3. Results and discussion

3.1. Experimental observation

Figs. 1b and c show the TEM images of the synthesized Si@C NPs under different magnifications. It can be seen that the Si@C NPs exhibit inhomogeneity in both the diameter of the Si core and the thickness of the carbon coating. *In situ* measurements indicate that the diameter of the Si core ranges from 10 to 150 nm while the carbon coating is about 5 to 15 nm in thickness. Moreover, the high resolution TEM image of a typical Si@C NP in Fig. 1d indicates that the carbon coating is amorphous, while the Si core is crystalline with high crystallinity confirmed by the selected area electron diffraction (SAED) pattern (Fig. 1e).

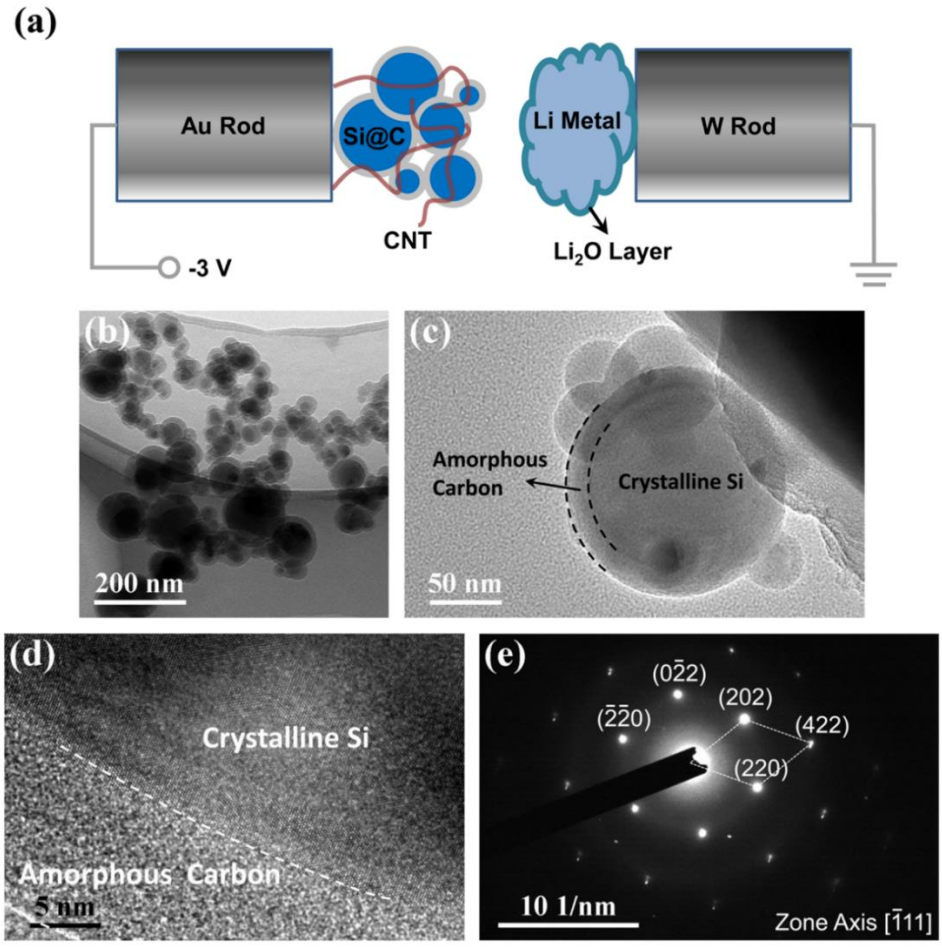

Fig. 1 (a) Schematic of the setup of *in situ* lithiation test; (b, c) TEM images of the Si@C NPs under different magnifications; (d) high resolution TEM image showing the amorphous carbon coating and the crystalline Si core as confirmed by the SAED pattern in (e).

Figs. 2a-f show the snapshots of the lithiation process of a Si@C NP with diameter of Si core about 60 nm and thickness of carbon coating around 9 nm. It was reported that bare crystalline Si NP with diameter smaller than 150 nm will not fracture during lithiation.[5] Unexpectedly, our *in situ* lithiation test showed that Si@C NP tends to fracture during lithiation even though the diameter of the Si core is only 60 nm. That is, carbon coating induces, rather than inhibits, the fracture of Si core and therefore plays a deleterious role in maintaining the integrity of Si@C NP during lithiation.

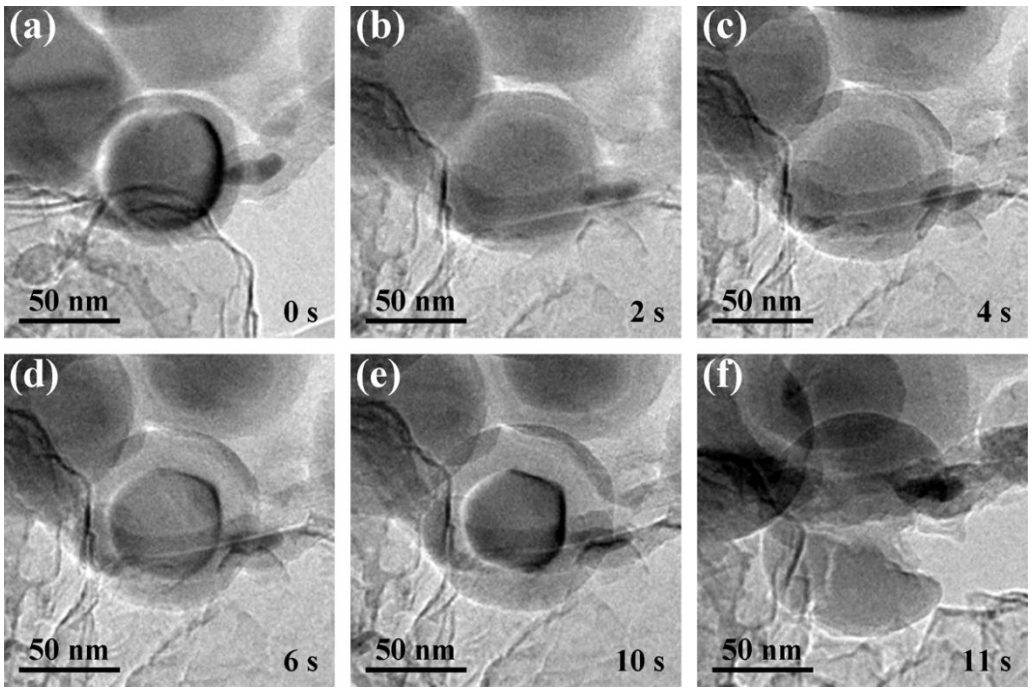

Fig. 2 Temporal evolution of the morphology of Si@C NP during *in situ* lithiation.

We repeated the *in situ* lithiation test on many Si@C NPs and found that lithiation may not necessarily lead to the fracture of Si@C NPs. Fig. 3 summarizes the events with

and without fracture on a *D*-*t* plane for all the tested Si@C NPs, where *D* refers to the diameter of the Si core and *t* stands for the thickness of the carbon coating. It can be seen that whether the Si@C NPs fracture or not after lithiation depends not only on the diameter of the Si core but also on the thickness of the carbon coating. A general trend implied by Fig. 3 is that Si@C NPs with larger *D* and smaller *t* tend to fracture during lithiation. Further examination on Fig. 3 indicates that the ratio between *D* and *t* may play an essential role in dominating the occurrence of fracture because fracture happens in all Si@C NPs with $D/t > 7.0$ while no fracture is observed in any Si@C NP with $D/t < 3.5$. For the Si@C NPs with intermediate *D*/*t* ranging from 3.5 to 7.0, the occurrence of fracture seems random. It can be inferred that there exists a critical ratio of *D*/*t*, below which fracture of Si@C NP can be prohibited. A rough estimation of such critical ratio of *D*/*t* obtained from Fig. 3 is a number between 3.5 and 7.0.

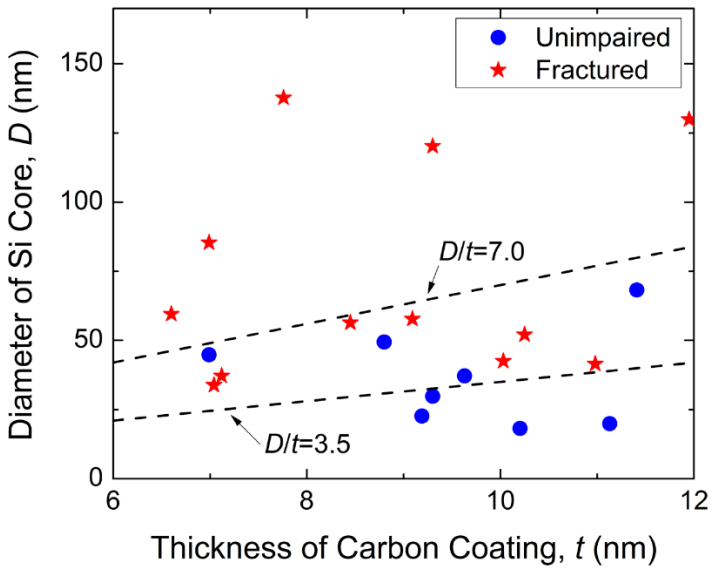

Fig. 3 Dependence of fracture of Si@C NP on the diameter of Si core and thickness of carbon coating.

3.2. Finite element analysis

In order to shed light on the fracture mechanism of Si@C NPs during lithiation especially for those with diameters much smaller than 150 nm, finite element analysis (FEA) was carried out. Fig. 4a shows the FEA model we applied, in which a Si@C NP (2-D) consists of a Si core with diameter of 100 nm and carbon coating with thickness of 5 nm. We firstly examined the stress developed in the carbon coating during lithiation. By following the approach of analogy we developed in our earlier work,[19] the lithiation-induced volume expansion can be equivalently treated as thermal expansion caused by a prescribed increment of the temperature field simulating the increase of Li^+ concentration. We neglected the lithiation of the carbon coating and assumed that the lithiation of Si core starts from its external periphery and advances symmetrically towards its center. The frontier of the lithiated region was assumed sharp.[22-25] That is, the core was either pristine (unlithiated) Si or fully lithiated Si (Li_xSi). We assumed that the carbon coating was pure elastic while the Si and Li_xSi were elastic-perfectly-plastic with mechanical properties taken as the values shown in Table 1. The Si and carbon coating were assumed perfectly bonded and no delamination was allowed on their interface. This assumption was based on our observation that no delamination happened between lithiated Si and carbon during *in situ* lithiation experiments. Such strong interfacial bonding between lithiated Si and carbon has also been reported in literature[11] and may be due to the interpenetration of Si and carbon near their interface as shown in Fig. 1d.

Table 1. Typical mechanical properties taken in FEA simulations

Materials	Young's modulus (GPa)	Poisson's ratio	Yield strength (GPa)
Carbon	300[26]	0.25[26]	-
Si	169[27]	0.26[27]	7[28]
Li_xSi	3.5[29]	0.23[30]	0.5[31,32]

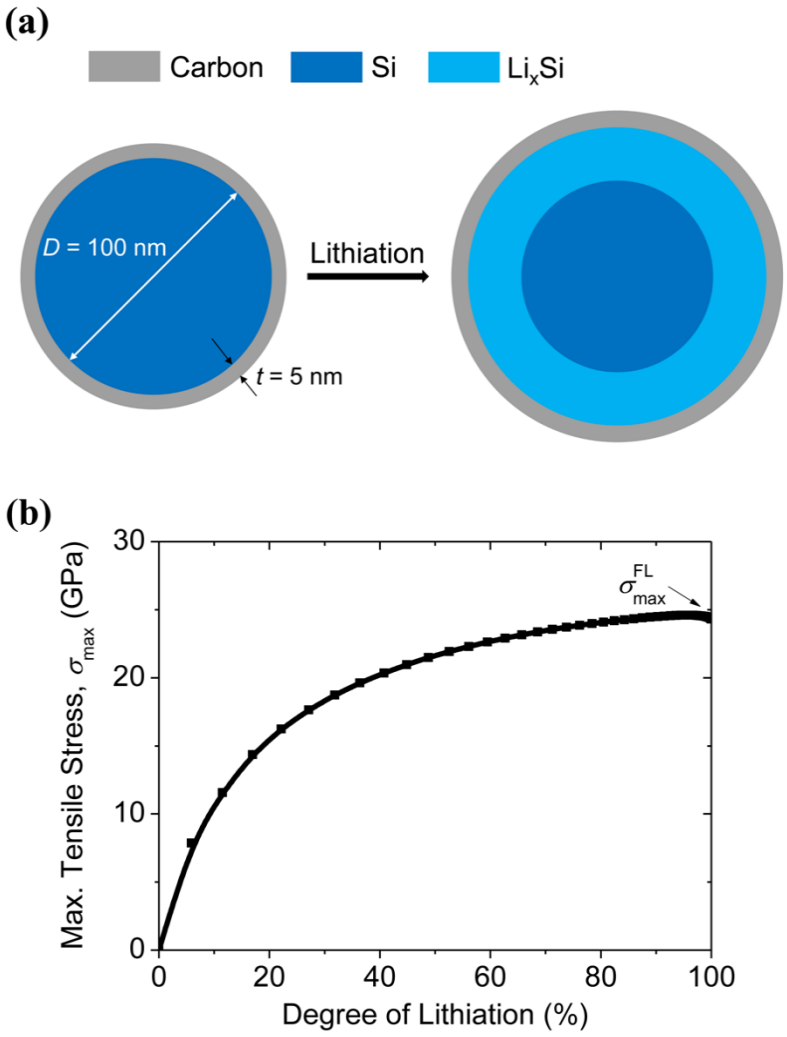

Fig. 4 (a) Schematic of FEA model of Si@C NP for evaluating the stress developed in the carbon coating during lithiation; (b) Variation of the maximum tensile stress (σ_{max}) in the carbon coating of Si@C NP with lithiation. σ_{max}^{FL} here denotes the maximum tensile stress in the carbon coating at the full lithiation moment.

To simulate the process of lithiation, the Si core was discretized into many concentric thin annuluses. Prescribed incremental "temperature" was applied on these thin annuluses one after another in the order from outside to inside, modelling the inward diffusion of the Li^+. The calculated results were found dependent on the number of the discrete annuluses or the annulus thickness, but convergent results can be obtained if the

thickness of the discrete annuluses is made sufficiently thin (Fig. S1†). Fig. 4b shows the evolution of the calculated maximum tensile stress, σ_{max}, in the carbon coating, which is along the hoop direction and is located near the carbon/Li_xSi interface, with the degree of lithiation. Here, degree of lithiation is defined as the fraction of the Si that has been lithiated. That is, 100% lithiation means fully lithiated. Fig. 4b indicates that the σ_{max} in the carbon coating increases with the degree of lithiation and almost saturates at ~25 GPa after 80% lithiation. According to the maximum-tensile-stress criterion of fracture for brittle materials,[33] the carbon coating will fracture if the σ_{max} reaches its fracture strength σ_f. For amorphous carbon, it was reported that σ_f ranges from 7 to 30 GPa.[26,34] If we take 7 GPa as a conservative estimation, Fig. 4b implies that fracture may take place around 6% lithiation.

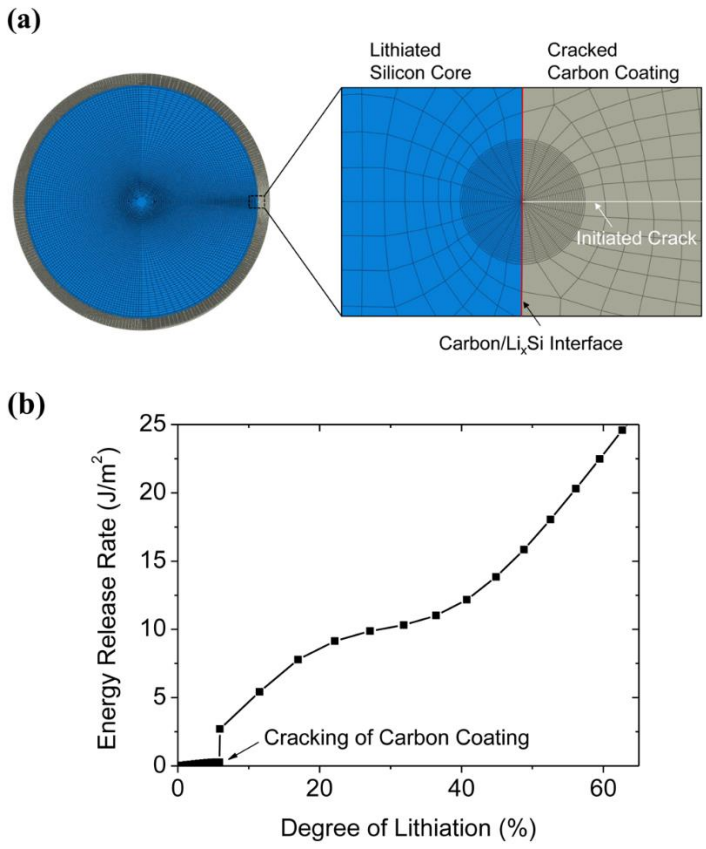

Fig. 5 (a) Meshed finite element model for calculating the energy release rate (*J*-integral) near the tip of a crack terminating at the carbon/lithiated Si interface; (b) Calculated energy release rate (*J*-integral) as a function of the degree of lithiation.

Once the carbon coating is fractured, a crack terminating at the carbon/Li_xSi interface forms. As the bonding between the lithiated Si and carbon is normally strong,[11] the formed crack is prone to penetrating into the lithiated Si rather than deflecting along the carbon/lithiated Si interface. To estimate the subsequent evolution of the crack, driving force for crack propagation was examined by calculating the *J*-integral[35] around the crack tip, as shown in Fig. 5a. The calculated evolution of the *J*-integral with the lithiation is shown in Fig. 5b. Based on the preceding analysis of the σ_{max} developed in the carbon coating, the cracking of carbon coating happens at the moment of 6% lithiation. Therefore, substantial *J*-integral is only observed after 6% lithiation. It can be seen that the *J*-integral increases rapidly with lithiation. It reaches up to more than 10 J m^{-2} at ~30% lithiation. That is, the *J*-integral can reach a considerable level upon a small amount of further lithiation after the cracking of the carbon coating. Recalling that the critical energy release rate for crack growth, or the fracture toughness, for lithiated Si is about 10 J m^{-2},[36,37] the *J*-integral near the crack tip can easily exceed this value, leading to the penetration of crack into the core and therefore the fracture of the whole Si@C NP. Such high energy release rate is mainly due to the material's inhomogeneity along the direction of crack extension, namely the dissimilarity between the carbon coating and lithiated Si in mechanical properties.[38] Earlier analysis in fracture mechanics indicated that material inhomogeneity could lead to either a shielding or anti-shielding effect on the crack propagation, depending on the directionality of inhomogeneity. If the crack tends to propagate from stiff/hard material to compliant/soft material, the material inhomogeneity

would facilitate the crack propagation. On the contrary, if the crack tends to propagate from compliant/soft material to stiff/hard material, the material inhomogeneity would prohibit the crack propagation.[38] Clearly, our case belongs to the former scenario because the carbon coating is stiffer and harder compared to the lithiated Si. A comparison was made between the energy release rates developed in a cracked Si@C NP and a cracked uncoated Si NP during lithiation. The results (Fig. S2†) show that the energy release rate in the uncoated Si NP, which has no material inhomogeneity, is much lower than that in a Si@C NP shown above even though the NPs and the preexisting cracks have the same size. Therefore, the carbon coating on the Si@C NP, if fractured, will expedite the fracture of the whole Si@C NP.

It should be pointed out that in our simulation the calculated *J*-integrals were found to have certain path-dependence. At given lithiation level, the calculated *J*-integral decreases with the distance of the path from the crack tip (Fig. S3†). When the path is sufficient far away from the crack tip, convergent *J*-integral is obtained, which is taken as the energy release rate shown in Fig. 5b.

3.3. Optimal design of Si@C NP

Above analysis indicates that the crack in the carbon coating, once developed, is quite easy to propagate into the Si core. To prevent the Si@C NP from fracturing, the integrity of the carbon coating should be secured, which can be achieved by optimizing the geometries of the Si@C NP. By adopting different diameters of the Si core (D) and thicknesses of the carbon coating (t) in the FEA model shown in Fig. 4a, we conducted a parametric study on the effects of D and t on the $\sigma_{\max}^{\mathrm{FL}}$ developed in the carbon coating

during lithiation. Here $\sigma_{\max}^{\mathrm{FL}}$ refers to the maximum tensile stress in the carbon coating at the full lithiation moment, as illustrated in Fig. 4b. Fig. 6 shows the normalized $\sigma_{\max}^{\mathrm{FL}}$ as a function of *D* and *t*. It can be seen that larger *D* and smaller *t* result in higher $\sigma_{\max}^{\mathrm{FL}}$. This trend agrees well with the observation from the *in situ* lithiation that Si@C NPs with larger core diameter and thinner coating thickness tend to fracture more easily during lithiation (Fig. 3). To prevent the fracture of the carbon coating, one should control the $\sigma_{\max}^{\mathrm{FL}}$ below the fracture strength of carbon σ_{f}. For given σ_{f}, Fig. 6 implies an "unimpaired region" on the *D*-*t* plane in which the $\sigma_{\max}^{\mathrm{FL}}$ is lower than σ_{f} or the integrity of carbon coating can be ensured. For example, if we take $\sigma_{\mathrm{f}} = 6\,\mathrm{GPa}$ and $E_{\mathrm{C}} = 300\,\mathrm{GPa}$, the region below the contour line of $\sigma_{\max}^{\mathrm{FL}} / E_{\mathrm{C}} = 0.02$ in Fig. 6 is the "unimpaired region". Interestingly, it can be seen that the contour line of 0.02 in Fig. 6 almost coincides with the line defined by *D*/*t* = 3.5. Similarly, the contour line corresponding to $\sigma_{\max}^{\mathrm{FL}} / E_{\mathrm{C}} = 0.04$ is quite close to the line defined by *D*/*t* = 7.0. Comparing Fig. 6 and Fig. 3, it can be predicted that the fracture strength of the carbon coating in our Si@C NPs ranges from 6 to 12 GPa, which agrees well with the value reported in the literature.[34] This prediction also justifies our earlier selection of $\sigma_{\mathrm{f}} = 7\,\mathrm{GPa}$ when predicting the critical degree of lithiation causing fracture of carbon coating for the model in Fig. 4a.

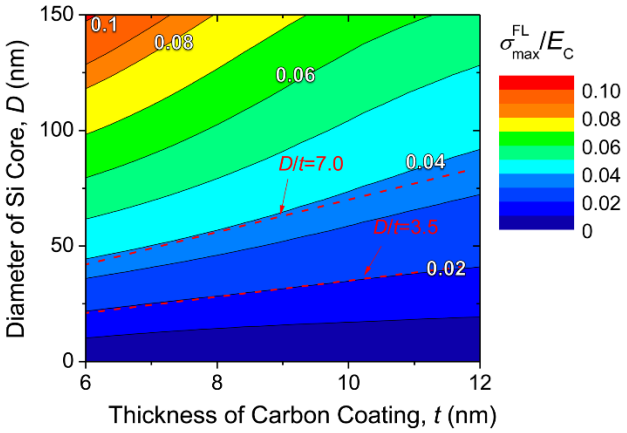

Fig. 6 Maximum tensile stress at full lithiation in the carbon coating of Si@C NPs with different core diameters *D* and coating thicknesses *t*. Here, σ_{max}^{FL} is normalized by E_C = 300 GPa.

Although Fig. 6 indicates that lower value of *D*/*t* is preferential for prohibiting the fracture of Si@C NPs, the demand for high capacity on the contrary requires higher *D*/*t* because Si possesses much higher theoretical capacity compared to carbon. The optimal value of *D*/*t* catering for both requirements above is the maximum mechanically allowable *D*/*t*. For our case, a conservative estimation of the optimal *D*/*t* from Fig. 6 is 3.5.

4. Conclusions

In this paper, *in situ* lithiation was carried out on the synthesized Si@C NPs. It was observed that lithiation could cause fracture of Si@C NPs with diameters smaller than 150 nm, which has been viewed as the maximum allowable size of bare Si nanoparticles immune to lithiation-induced fracture. Such deleterious effect of carbon coating on the integrity of Si@C NP was analyzed using FE simulation. Our results indicated that the

maximum tensile stress experienced by the carbon coating of Si@C NP during the lithiation process depends on the size of the Si core as well as the thickness of the carbon coating. Excessive tensile stress will be readily developed in the carbon coating if the Si core is too large or the carbon coating is too thin, leading to the fracture of the carbon coating. The resulting crack in the carbon coating will experience an elevated driving force for growth due to the unfavorable material inhomogeneity between the carbon coating and the lithiated Si, inducing the fracture of the whole Si@C NP. To secure the structural integrity of Si@C NP during lithiation and meanwhile attain capacity as high as possible, a design guideline for Si@C NP is proposed by controlling the ratio between the Si core diameter and the carbon coating thickness below a critical value. Our discussion above was based on the assumption that the carbon coating and lithiated Si were perfectly bonded. Recently, people developed slidable layered graphene coating on Si[12] and yolk-shell architecture,[10] in which the carbon/Si interface was weak or even vanishing. These innovations provide alternative solutions for solving the fracture problem of electrode materials during lithiation. Admittedly, our results provided a necessary but not a sufficient condition for the long cycle life of the Si@C NP electrode materials since we only considered the integrity of the carbon coating during the first lithiation. The fatigue stability of electrode materials upon cyclic lithiation and delithiation loading, the interactions between the electrode materials and the current collector and the formation and stability of SEI layers have not been considered fully and require further studies.

Acknowledgements

This work was supported by the General Research Fund from Hong Kong RGC (529313). HW would like to acknowledge the support from the National Natural Science Foundation of China (11322219, 11321202). WL acknowledges Mr. Zheng-Long Xu and Prof. Jang-Kyo Kim from the Hong Kong University of Science and Technology for the helpful discussion on the lithiation-induced fracture of Si@C nanoparticles, and Dr. Wei Lu from the Materials Research Center of the Hong Kong Polytechnic University for providing technical supports.

References

1 A. S. Aricò, P. Bruce, B. Scrosati, J.-M. Tarascon and W. van Schalkwijk, *Nat. Mater.*, 2005, **4**, 366-377.

2 M. T. McDowell, S. W. Lee, W. D. Nix and Y. Cui, *Adv. Mater.*, 2013, **25**, 4966-4985.

3 C. K. Chan, H. Peng, G. Liu, K. McIlwrath, X. F. Zhang, R. A. Huggins and Y. Cui, *Nat. Nanotechnol.*, 2008, **3**, 31-35.

4 X. H. Liu, H. Zheng, L. Zhong, S. Huang, K. Karki, L. Q. Zhang, Y. Liu, A. Kushima, W. T. Liang, J. W. Wang, J.-H. Cho, E. Epstein, S. A. Dayeh, S. T. Picraux, T. Zhu, J. Li, J. P. Sullivan, J. Cumings, C. Wang, S. X. Mao, Z. Z. Ye, S. Zhang and J. Y. Huang, *Nano Lett.*, 2011, **11**, 3312-3318.

5 X. H. Liu, L. Zhong, S. Huang, S. X. Mao, T. Zhu and J. Y. Huang, *ACS Nano*, 2012, **6**, 1522-1531.

6 M. T. McDowell, S. W. Lee, J. T. Harris, B. A. Korgel, C. Wang, W. D. Nix and Y. Cui, *Nano Lett.*, 2013, **13**, 758-764.

7 H. Wu, G. Chan, J. W. Choi, I. Ryu, Y. Yao, M. T. McDowell, S. W. Lee, A. Jackson, Y. Yang, L. Hu and Y. Cui, *Nat. Nanotechnol.*, 2012, **7**, 310-315.

8 S.-H. Ng, J. Wang, D. Wexler, K. Konstantinov, Z.-P. Guo and H.-K. Liu, *Angew. Chem. Int. Ed.*, 2006, **45**, 6896-6899.

9 M. Gu, Y. Li, X. Li, S. Hu, X. Zhang, W. Xu, S. Thevuthasan, D. R. Baer, J.-G. Zhang, J. Liu and C. Wang, *ACS Nano*, 2012, **6**, 8439-8447.

10 N. Liu, H. Wu, M. T. McDowell, Y. Yao, C. Wang and Y. Cui, *Nano Lett.*, 2012, **12**, 3315-3321.

11 M. E. Stournara, Y. Qi and V. B. Shenoy, *Nano Lett.*, 2014, **14**, 2140-2149.

12 I. H. Son, J. H. Park, S. Kwon, S. Park, M. H. Rümmeli, A. Bachmatiuk, H. J. Song, J. Ku, J. W. Choi, J.-m. Choi, S.-G. Doo and H. Chang, *Nat. Commun.*, 2015, **6**.

13 C.-M. Wang, X. Li, Z. Wang, W. Xu, J. Liu, F. Gao, L. Kovarik, J.-G. Zhang, J. Howe, D. J. Burton, Z. Liu, X. Xiao, S. Thevuthasan and D. R. Baer, *Nano Lett.*, 2012, **12**, 1624-1632.
14 L. Luo, H. Yang, P. Yan, J. J. Travis, Y. Lee, N. Liu, D. M. Piper, S.-H. Lee, P. Zhao, S. M. George, J.-G. Zhang, Y. Cui, S. Zhang, C. Ban and C.-M. Wang, *ACS Nano*, 2015, **9**, 5559-5566.
15 X. H. Liu, Y. Liu, A. Kushima, S. Zhang, T. Zhu, J. Li and J. Y. Huang, *Adv. Energy Mater.*, 2012, **2**, 722-741.
16 Q. Li, P. Wang, Q. Feng, M. Mao, J. Liu, S. X. Mao and H. Wang, *Chem. Mater.*, 2014, **26**, 4102-4108.
17 H. Yang, S. Huang, X. Huang, F. Fan, W. Liang, X. H. Liu, L.-Q. Chen, J. Y. Huang, J. Li, T. Zhu and S. Zhang, *Nano Lett.*, 2012, **12**, 1953-1958.
18 H. Yang, F. Fan, W. Liang, X. Guo, T. Zhu and S. Zhang, *J. Mech. Phys. Solids*, 2014, **70**, 349-361.
19 Q. Li, W. Li, Q. Feng, P. Wang, M. Mao, J. Liu, L. Zhou, H. Wang and H. Yao, *Carbon*, 2014, **80**, 793-798.
20 X.-Y. Zhou, J.-J. Tang, J. Yang, J. Xie and L.-L. Ma, *Electrochim. Acta*, 2013, **87**, 663-668.
21 M. N. Obrovac and L. Christensen, *Electrochem. Solid-State Lett.*, 2004, **7**, A93-A96.
22 M. T. McDowell, I. Ryu, S. W. Lee, C. Wang, W. D. Nix and Y. Cui, *Adv. Mater.*, 2012, **24**, 6034-6041.
23 X. H. Liu, J. W. Wang, S. Huang, F. Fan, X. Huang, Y. Liu, S. Krylyuk, J. Yoo, S. A. Dayeh, A. V. Davydov, S. X. Mao, S. T. Picraux, S. Zhang, J. Li, T. Zhu and J. Y. Huang, *Nat. Nanotechnol.*, 2012, **7**, 749-756.
24 K. Karki, E. Epstein, J.-H. Cho, Z. Jia, T. Li, S. T. Picraux, C. Wang and J. Cumings, *Nano Lett.*, 2012, **12**, 1392-1397.
25 J. W. Wang, Y. He, F. Fan, X. H. Liu, S. Xia, Y. Liu, C. T. Harris, H. Li, J. Y. Huang, S. X. Mao and T. Zhu, *Nano Lett.*, 2013, **13**, 709-715.
26 M. G. Fyta, I. N. Remediakis, P. C. Kelires and D. A. Papaconstantopoulos, *Phys. Rev. Lett.*, 2006, **96**, 185503.
27 W. A. Brantley, *J. Appl. Phys.*, 1973, **44**, 534-535.
28 K. E. Petersen, *Proc. IEEE*, 1982, **70**, 420-457.
29 A. Kushima, J. Y. Huang and J. Li, *ACS Nano*, 2012, **6**, 9425-9432.
30 V. B. Shenoy, P. Johari and Y. Qi, *J. Power Sources*, 2010, **195**, 6825-6830.
31 M. J. Chon, V. A. Sethuraman, A. McCormick, V. Srinivasan and P. R. Guduru, *Phys. Rev. Lett.*, 2011, **107**, 045503.
32 S. K. Soni, B. W. Sheldon, X. Xiao, M. W. Verbrugge, D. Ahn, H. Haftbaradaran and H. Gao, *J. Electrochem. Soc.*, 2012, **159**, A38-A43.
33 M. A. Meyers and K. K. Chawla, *Mechanical Behavior of Materials*, Cambridge University Press, New York, 2009.
34 S. Cho, I. Chasiotis, T. A. Friedmann and J. P. Sullivan, *J. Micromech. Microeng.*, 2005, **15**, 728-735.
35 T. L. Anderson, *Fracture Mechanics: Fundamentals and Applications*, CRC Press, Boca Raton, 2005.

353 36 K. Zhao, M. Pharr, Q. Wan, W. L. Wang, E. Kaxiras, J. J. Vlassak and Z. Suo, *J.*
354 *Electrochem. Soc.*, 2012, **159**, A238-A243.
355 37 M. Pharr, Z. Suo and J. J. Vlassak, *Nano Lett.*, 2013, **13**, 5570-5577.
356 38 N. K. Simha, F. D. Fischer, O. Kolednik and C. R. Chen, *J. Mech. Phys. Solids*,
357 2003, **51**, 209-240.